Biochemical and Biophysical Research Communications 460 (2015) 530–536

Contents lists available at ScienceDirect

Biochemical and Biophysical Research Communications

journal homepage: www.elsevier.com/locate/ybbrc

IRE1α-TRAF2-ASK1 complex-mediated endoplasmic reticulum stress and mitochondrial dysfunction contribute to CXC195-induced apoptosis in human bladder carcinoma T24 cells

Tao Zeng [a, *, 1], Lifen Peng [c, 1], Haichao Chao [a], Haibo Xi [d], Bin Fu [d], Yibing Wang [d], Zunwei Zhu [b], Gongxian Wang [d]

[a] School of Medicine, Nanchang University, Nanchang, Jiangxi, PR China
[b] Department of Urology, The People's Hospital of Jiangxi Province, Nanchang, PR China
[c] E.N.T. Department, The People's Hospital of Jiangxi Province, Nanchang, PR China
[d] Institute of Urology, The First Affiliated Hospital of Nanchang University, Nanchang, Jiangxi, PR China

ARTICLE INFO

Article history:
Received 2 March 2015
Available online 19 March 2015

Keywords:
Bladder urothelial carcinoma
CXC195
Apoptosis
IRE1a-TRAF2-ASK1 complex
ER stress
JNK

ABSTRACT

Bladder urothelial carcinoma (UC) accounts for approximately 5% of all cancer deaths in humans. Current treatments extend the recurrence interval but do not significantly alter patient survival. The objective of the present study was to investigate the anti-cancer effect and the underlying mechanisms of CXC195 against human UC cell line T24 cells. CXC195 inhibited the cells growth and induced caspase- and mitochondrial-dependent apoptosis in T24 cells. In addition, CXC195 triggered activation of proteins involved in ER stress signaling including GRP78, CHOP, IRE1α, TRAF2, p-ASK1 and p-JNK in T24 cells. Co-immunoprecipitation experiments showed that activation of JNK was induced by the activation of IRE1α through formation of an IRE1α-TRAF2-ASK1 complex. Knockdown of IRE1α by siRNA dramatically abrogated CXC195-induced activation of TRAF2, ASK and JNK, formation of an IRE1α-TRAF2-ASK1 complex and caspase- and mitochondrial-dependent apoptosis in T24 cells. These findings provided new insights to understand the mode of action of CXC195 in treatment of human UC.

1. Introduction

Bladder urothelial carcinoma (UC) ranks fourth in incidence among cancers in men and eighth in women in the United States [1]. Despite recent advances in surgical and chemotherapeutic procedures, the 5-year survival rate in patients with invasive and metastatic bladder cancer remains very low [2]. Intravesical chemotherapy is one of the most direct ways to reduce recurrence and mortality. Unfortunately, these chemical agents commonly produce severe side effects, including urinary frequency, urinary urgency, cystitis, and hematuria [3]. Therefore, there is an urgent need to explore drugs that are both effective and non-toxic for UC.

Apoptosis is a major method of anti-cancer properties to eliminate cancer cells. The understanding of apoptosis has provided the basis for novel targeted therapies that can induce death in cancer cells or sensitize them to established cytotoxic agents [4]. Up to now, apoptosis occurs via three separate yet interlinked signaling mechanisms: death receptor-mediated extrinsic pathway [5], mitochondria-mediated intrinsic pathway [6] and endoplasmic reticulum (ER) stress-mediated apoptotic pathway [7]. Thus, targeting apoptosis pathways in premalignant and malignant cells may be an effective strategy for cancer prevention and treatment.

Tetramethylpyrazine (TMP), one of the major bioactive components purified from the Chinese herb Chuanxiong (*Ligusticum wallichi Franchat*), have shown a wide variety of anti-tumor effects [8–11] and a lot of attention has been drawn to further development of its analog [12]. CXC195 is a TMP analog showing the antioxidant activity and anti-apoptotic effect in transient focal ischemia via inhibiting NADPH Oxidase and iNOS expression [13] and regulating PI3K-AKT-GSK3β pathway [14]. In addition, CXC195 could prevent human umbilical vein endothelial cells (HUVECs) from H_2O_2-induced apoptosis through inhibition of the mitochondria- and caspase-dependent pathway [15]. Recent study showed that CXC195 could inhibit cell proliferation and inflammatory response

* Corresponding author Department of Urology, the People's Hospital of Jiangxi Province, Nanchang, PR China
E-mail address: zengtaonanchang@163.com (T. Zeng).
[1] Tao Zeng and Lifen Peng contributed equally to this work.

http://dx.doi.org/10.1016/j.bbrc.2015.03.064
0006-291X/

in LPS-induced human hepatocellular carcinoma HepG2 cells through inhibiting the TLR4-MyD88-TAK1 mediated NF-κB and MAPK signaling pathway activation [16]. Therefore, CXC195 is thought to be a valuable anti-cancer medicine; however, cellular and molecular mechanisms underlying the anti-cancer effects of CXC195 has not yet been clarified.

In the present study, we demonstrated that CXC195 was a potent anti-cancer agent against human UC T24 cells, and IRE1α-TRAF2-ASK1 complex-mediated ER stress and mitochondrial dysfunction might be involved in the signaling of CXC195-induced apoptosis. Our data provide the molecular theoretical basis for clinical application of CXC195 in patients with UC.

2. Materials and methods

2.1. Cell culture and treatment

The human UC T24 cells line (Meixuan Biotechnological Company, Shanghai, China) were cultured in McCoy's medium and modified Eagle's medium (Life Technologies, Carlsbad, CA, USA) containing 10% fetal calf serum (HyClone, Logan, UT, USA) and 50 mg/ml penicillin/streptomycin (Sigma, St. Louis, MO, USA), and was maintained at 37 °C and 5% CO_2. At 80% confluency, the cells were treated with increasing concentrations (0, 40, 80, 120 and 160 μM) for 24 h or 160 μM CXC195 for various periods (0 h, 12 h, 24 h, 48 h or 96 h). CXC195 (Fig. 1A) was synthesized by 2-chloromethyl-3, 5, 6-trimethylpyrazine hydrochloride directly reacting with the 4, 4′-difluorobenzhydrylpiperazine. Its purity (>98%) was determined by high-performance liquid chromatography. The tested compounds and positive control were dissolved in DMSO.

2.1.1. Cell viability assay

The effect of CXC195 on the cell viability of T24 cells was evaluated in vitro using the MTT assay (Sigma). Briefly, 1×10^5 cells were seeded into 96-well plates. After treatment with CXC195, 5 mg/ml MTT (15 μl/well) was added to the cells. Then the culture medium was removed and 150 ml of DMSO was added to each well. The plates were shaken on a swing bed for 10 min, and the optical density was detected using an enzyme-linked immunosorbent assay plate reader at 490 nm. Percent inhibition of cytotoxicity was calculated as a fraction of control (with DMSO) and expressed as percentage of cell viability.

2.1.2. Double staining for annexin V-FITC and propidium iodide (PI)

Briefly, T24 cells were trypsinized and washed twice with PBS, centrifuged at 800 rpm for 5 min. Then, 1×10^6 cells were suspended in binding buffer and double-stained with Annexin V-FITC and PI for 30 min at room temperature. After that, the fluorescence of each sample was quantitatively analyzed by FACS calibur flow cytometer and CellQuest software.

2.1.3. Caspase activity assay

The activities of caspase3 and caspase9 were determined according to the manufacturer's instructions (Beyotime Company, Shanghai, China). Cell lysates (30 μg) from T24 cells were determined spectrophotometrically at 405 nm using a microtiter plate reader. The assays were performed by incubating the cell lysates with 0.2 mM of the caspase-specific colorimetric tetrapeptide substrates, Ac-LEHD-p-nitroaniline (pNA) (for caspase9) or Ac-DEVD-pNA (for caspase3) for 1 h at 37 °C. The increase in the absorbance at 405 nm which corresponds to the amount of pNA liberated from the peptide substrates was converted into units of enzyme activity using a standard curve generated with free pNA. One unit of caspase3 or caspase9 activity correspond to the amount of enzyme that will release 1 pmol of pNA from 0.2 mM DEVD-pNA, IETD-pNA or Ac-LEHD-pNA per min, respectively.

2.1.4. Cytochrome c (Cyt c) release

T24 cells were collected by centrifugation at 800 rpm for 5 min at 48 °C and washed with ice-cold PBS. Cell nuclear and cytoplasmic fractions were prepared using a nuclear/cytosol fractionation kit of Biovision Inc. (Moutain View, CA) according to the manufacture's direction. The fractionation of the mitochondrial protein and

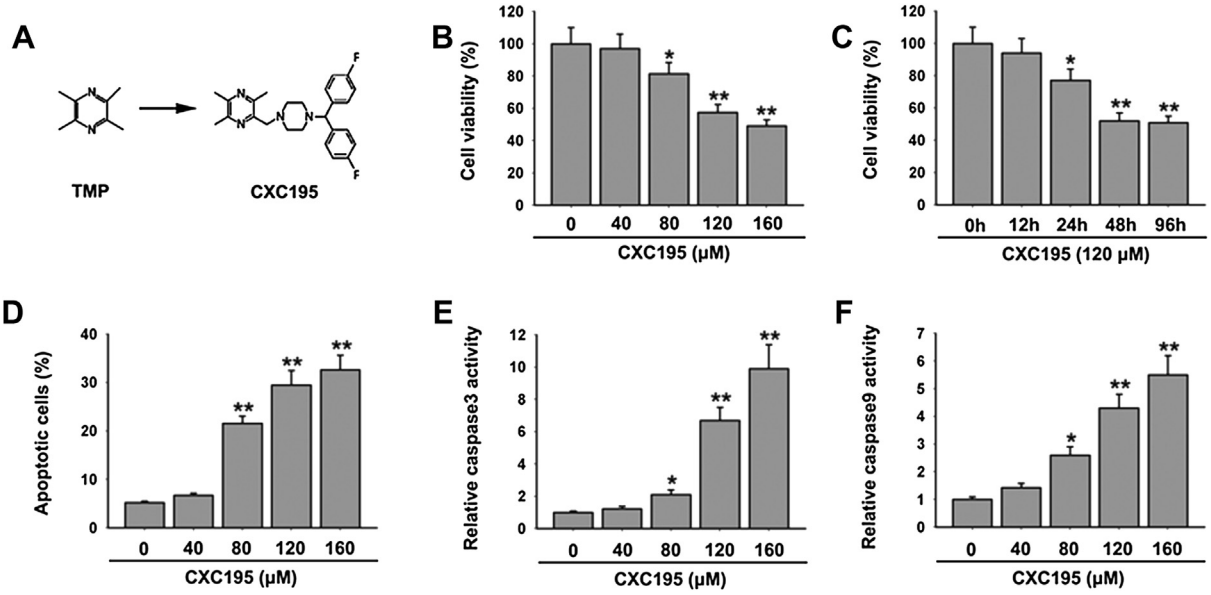

Fig. 1. Effects of CXC195 on the cell viability and apoptosis of T24 cells. (A). Chemical structures of CXC195. Cell viability was assayed by the MTT assay. (B). Effect of different concentrations of CXC195 on the cell viability of T24 cells. The control group set at 100%. (C). Effect of 160 μM CXC195 on the cell viability of T24 cells in a time-dependent manner. T24 cells treated with 160 μM CXC195 for 0 h set at 100%. (D). Effect of 160 μM CXC195 on the apoptotic rate of T24 cells. Cells were analyzed by flow cytometry after staining with Annexin-V and PI. (E–F). The activation of caspase3 and caspase9 was measured in T24 cells after treatment with different concentrations of CXC195 for 48 h. All data are presented as means ± SD. (n = 6, *P < 0.05, **P < 0.01 significantly different from the control group).

cytosolic protein were extracted according to the instruction of Mitochondrial Protein Extraction kit (KeyGen), respectively. After centrifugation, the supernatants were obtained for western blot analysis.

2.1.5. Immunoprecipitation (IP)

To examine protein–protein interactions, T24 cells were lysed in 1 ml buffer consisting of 50 mM Trise HCl (pH 7.4), 150 mM NaCl, 1% Triton X-100, 0.5% sodium deoxycholate, 10 mM NaF, 1 mM Na_3VO_4, 10 g/ml leupeptin, 10 g/ml aprotinin and 20 mM PMSF after harvesting. Aliquots of the cellular lysates (containing 500 μg proteins) were incubated with proper primary anti-IRE1α antibodies with rocking overnight at 4 °C. The immune complexes were allowed to bind to 40 μl of Recombinant Protein G Agarose beads (Invitrogen, USA) at 4 °C for 2 h, and the beads were washed three times with lysis buffer. The washed beads were re-suspended in electrophoresis sample buffer and boiled for 10 min. After centrifugation, the supernatants were obtained as immunoprecipitates for western blot analysis.

2.1.6. Western blot analysis

Protein samples from T24 cells extracts were separated by 8% or 10% SDS-PAGE and transferred to a nitrocellulose membrane (Amersham Pharmacia Biotech, Buck-inghamshire, UK). The membrane was blocked with 5% skim milk and incubated with primary antibodies, which were purchased from these companies. Santa Cruz: Cyt *c*, COX4, β-Tubulin, death protein 5 (DP5), p53-upregulated modulator of apoptosis (PUMA) and β-actin; Cell Signaling: inositol-requiring protein1α (IRE1α), IRE1-tumor necrosis factor receptor-associated factor 2 (TRAF2), activated apoptosis signal-regulating kinase 1 (ASK) and c-Jun N-terminal kinase (JNK). After washing with TBST, HRP-conjugated secondary antibodies (goat anti-rabbit IgG and donkey anti-mouse IgG, Santa Cruz Biotechnology) were applied. The blots were developed using ECL Western Blotting Detection Reagents (Amersham Pharmacia Biotech). Densitometry analysis of bands was performed with the Image Master™ 2D Elite software, version 3.1 (Amersham Pharmacia Biotech).

2.1.7. Reverse transcription-polymerase chain reaction (RT-PCR)

Total messenger RNA from T24 cells was isolated using RNeasy mini kit (Qiagen, Valencia, CA, USA) according to the manufacturer's instructions. The amount and quality of the RNA were determined using a NanoDrop 2000 Spectrophotometer (Thermo Scientific, Wilmington, DE, USA). First-strand cDNA was synthesized from 300 ng RNA with SuperScript® III First-Strand Synthesis System (Applied Biosystems, Foster City, CA, USA) and used as the template for PCR with the FastStart High Fidelity PCR System (Roche Applied Science, Indianapolis, IN, USA). The primers of target genes were as follows in Table 1. The PCR products were resolved using a 1% agarose gel containing GelRed, and the relationship between the amount of PCR product and the number of amplification cycles was linear (data not shown).

2.1.8. Small RNA interference (siRNA)

T24 cells were seeded at 1×10^5 cells/well in 24-well plates and allowed to reach approximately 50% confluence on the day of transfection. The siRNA constructs used were obtained as the siGENOME SMARTpool reagents (Dharmacon, Lafayette, CO), the siGENOME SMARTpool IRE1α (M-004951-01-0010). The non-targeting siRNA control, SiConTRolNon-targeting SiRNA pool (D-001206-13-20) was also obtained from Dharmacon. Cells were transfected with 50–100 nM siRNA in Opti-MEM medium (Invitrogen, Carlsbad, CA) with 5% fetal calf serum using Lipofectamine reagent (Invitrogen, Carlsbad, CA) according to the manufacturer's transfection protocol. Twenty-four hours after transfection, the cells were treated with or without CXC195 for the indicated time point before the subsequent experiments. Efficiency of siRNA was measured by western blot analysis.

2.1.9. Statistical analysis

Statistical calculations of the data were performed using an unpaired Student's t-test and ANOVA analysis. Statistical significance was at $P < 0.05$.

3. Results

3.1. CXC195 induced cytotoxicity and apoptosis in T24 cells

Fig. 1B and C showed that CXC195 efficiently decreased the cell viability of T24 cells in a concentration- and time-dependent manner. At the highest concentration of CXC195 (160 μM), 48–96 h treatment decreased cell viability by approximately 50% in T24 cells (Fig. 1C). Annexin V/PI binding was used to evaluate the effect of CXC195 on T24 cells death. Treatment with CXC195 for 48 h resulted in an increase in the apoptotic ratio of T24 cells in a concentration-dependent manner, which markedly increased up to 34% at the highest concentration of CXC195 (160 μM) (Fig. 1D). Apoptosis induced by various cytotoxic agents is highly dependent on the activation of caspases, which play pivotal roles in cleaving specific target proteins. Therefore, we assessed whether CXC195 activated caspase pathways in T24 cells. As shown in Fig. 1E and F, CXC195 triggered a specific activities of caspase3 and caspas9 after incubating T24 cells with CXC195 in a concentration-dependent manner for 48 h.

3.2. CXC195 induced apoptosis of T24 cells on the mitochondrial-dependent pathway

The release of pro-apoptotic proteins such as Cyt *c* from the inter-membrane space to the cytosol is required for caspase activation that initiates the apoptotic program [17]. Western blot analysis showed that Cyt *c* gradually accumulated in the cytosol, whereas the protein levels of Cyt *c* in the mitochondria progressively decreased in T24 cells after treatment with various concentrations of CXC195 for 48 h (Fig. 2A–C).

Since Bcl-2 family proteins were known to control mitochondria-mediated apoptosis pathway by maintaining a balance between pro- and anti-apoptotic members [6], we examined the effects of CXC195 on the expression levels of Bcl-2 family proteins in T24 cells. Our results showed that CXC195 increased the mRNA level of pro-apoptotic Bax (Fig. 2D), but decreased the mRNA levels of anti-apoptotic Bcl-2 and Bcl-XL (Fig. 2E–F) in T24 cells.

The other pro-apoptotic molecules, the BH3-only proteins, such as death protein 5 (DP5) and p53-upregulated modulator of apoptosis (PUMA), are the initiators of mitochondrial apoptosis [18,19]. They are activated by a variety of cellular stresses and in turn directly or indirectly activate the Bax-like proteins. Our results showed that CXC195 also increased the protein levels of PUMA and DP5 in T24 cells (Fig. 2G–I). These results indicated that CXC195 triggered apoptosis through the intrinsic mitochondrial-dependent pathway, after mitochondrial dysfunction and Cyt *c* release in T24 cells.

3.3. CXC195 induced ER stress in T24 cells

There is increasing evidence that ER stress plays a crucial role in the regulation of apoptosis [7]. To confirm the hypothesis that the ER stress played a role in mediating the apoptosis of CXC195, we examined the effect of CXC195 on the expression of ER stress-associated proteins: glucose-regulated protein of 78 kDa (GRP78)

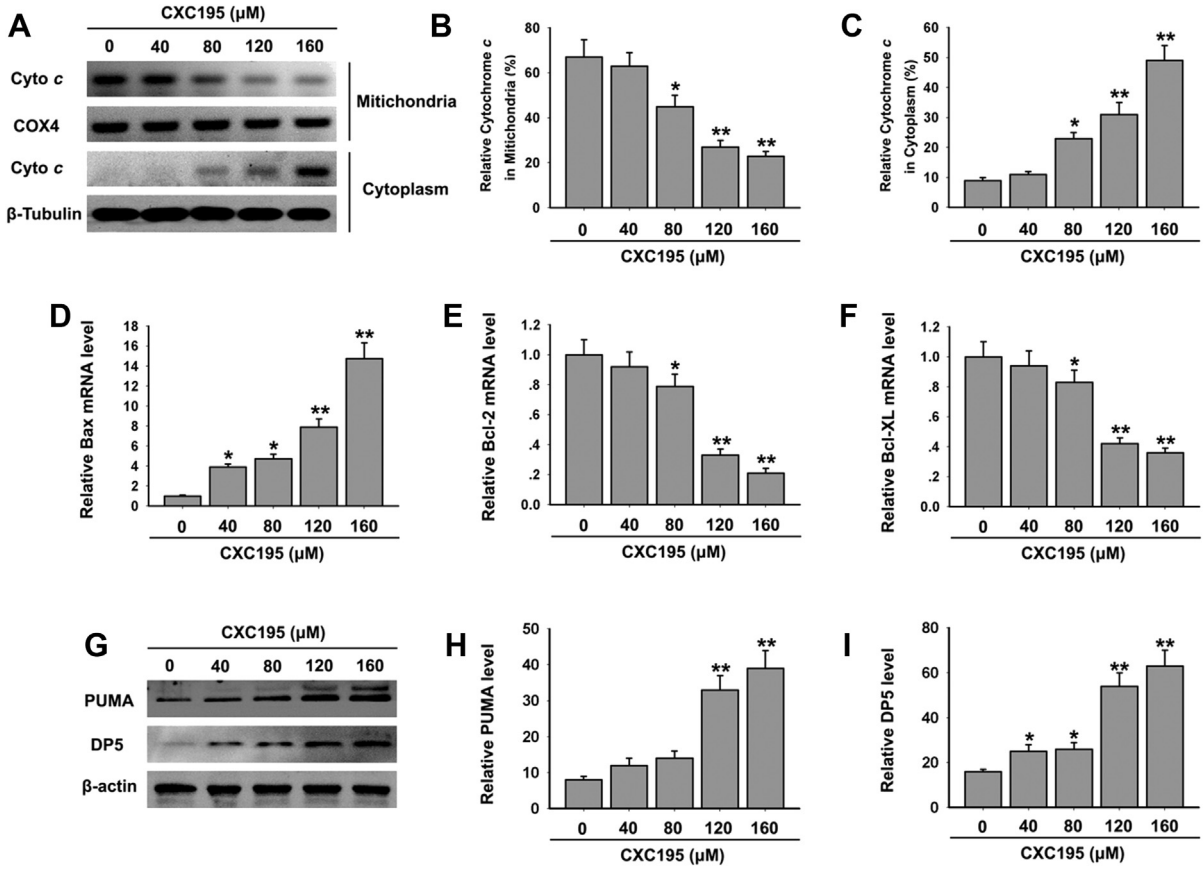

Fig. 2. Effect of CXC195 on the activation of mitochondrial-dependent apoptotic signaling in T24 cells. T24 cells were treated with different concentrations of CXC195 for 48 h (A). The levels of Cyto *c* in both mitochondrial and cytosolic fractions was measured by western blotting assay. Expression of COX-4 and Tubulin was used for monitoring mitochondrial release of cytochrome c into the cytosol. (B–C). The bar chart showed the ratio of Cyto *c* to COX-4 in mitochondrial and β-Tubulin in cytosolic fractions at each group. (D–F). The mRNA levels of Bax, Bcl-2 and Bcl-XL were measured by RT-PCR. (G). The protein levels of PUMA and DP5 were measured by western blot analysis. (H–I). The bar chart showed the ratio of PUMA and DP5 to β-actin at each group. These data are means ± SEM. (n = 6, $^{*}P < 0.05$, $^{**}P < 0.01$ significantly different from the control group).

and CCAAT/enhancer-binding protein homologous protein (CHOP) in T24 cells. RT-PCR results showed mRNA levels of GRP78 and CHOP increased in T24 cells after treatment with various concentrations of CXC195 for 48 h (Fig. 3A–B).

3.4. CXC195 increased IRE1α and TRAF2 expression, and activated ASK1 and JNK in T24 cells

Previous studies have shown that the JNK signaling pathway could be activated by ER stress following recruitment of TRAF2 by the IRE1α cytosolic kinase to form a TRAF2-ASK1-IRE1 complex [7]. As depicted in Fig. 3C–E, increased expression of IRE1α, TRAF2, p-ASK and p-JNK was markedly measured in T24 cells after treatment with various concentrations of CXC195 for 48 h. To further explore the role of ER stress in CXC195-induced apoptosis, T24 cells were transfected with or without IRE1α siRNA for 24 h. Twenty-four hours later, T24 cells were treated with CXC195 for 48 h. As shown in Fig. 3F–H, siRNA knockdown of IRE1α markedly inhibited its up-regulation by CXC195 (160 μM) in T24 cells. Furthermore, inhibition of IRE1α also markedly inhibited up-regulation of TRAF2, p-ASK and p-JNK in CXC195-induced T24 cells.

3.5. CXC195 increased the interactions of IRE1α with TRAF2 or ASK in T24 cells

To assess the possible interaction of IRE1α with TRAF2 or ASK, we treated T24 cells with or without CXC195 (160 μM) for 48 h. As shown in Fig. 3I–J, when cell lysates were immunoprecipitated with anti-IRE1α antibody and immunoblotted with anti-TRAF2 and anti-ASK1 antibody, TRAF2 and ASK1 were found to be associated with IRE1α after treatment with CXC195. siRNA knockdown of IRE1α markedly inhibited its association with TRAF2 and ASK1 in CXC195 (160 μM) treated T24 cells.

3.6. IRE1α is required for CXC195-induced apoptosis in T24 cells

To confirm the requirement of IRE1α for CXC195-induced apoptosis, we transfected with IRE1α siRNA following treatment with CXC195. The cell viability up-regulated by approximately 19% (Fig. 4A) and the apoptotic ratio down-regulated by approximately 21% (Fig. 4B) compared with CXC195 treatment group. In addition, the activation of caspase3 and 9 was markedly inhibited in IRE1α siRNA transfected T24 cells (Fig. 4C). Moreover, inhibition of IRE1α markedly inhibited expression of pro-apoptotic molecules (Bax, PUMA and DP5) and increased expression of anti-apoptotic molecules (Bcl-2 and Bcl-XL) in T24 cells compared with CXC195 treatment group (Fig. 4D–G).

4. Discussion

CXC195 are known as a TMP analog and have the antioxidant activity and anti-apoptotic effect in neuron [13,14] and HUVECs [15]. Recent studies have shown that CXC195 inhibit proliferation and inflammatory response of LPS-induced human hepatocellular

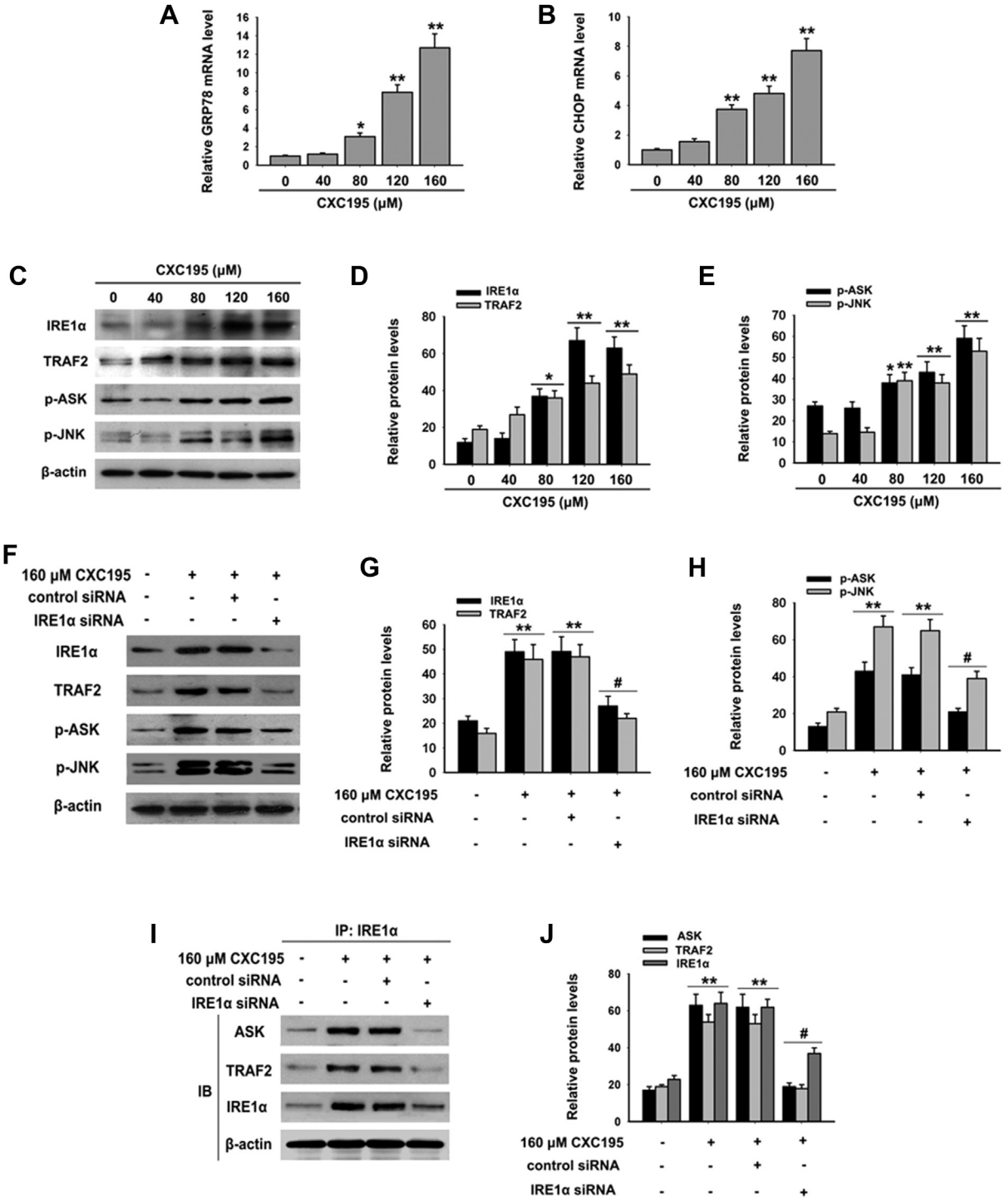

Fig. 3. Effect of CXC195 on the ER stress and IRE1α-dependent pathway in T24 cells. T24 cells were treated with different concentrations of CXC195 for 48 h (A–B). The mRNA levels of GRP78 and CHOP were measured by RT-PCR. (C). The protein levels of IRE1α, TRAF2, p-ASK1 and p-JNK were measured by western blot analysis. (D–E). The bar chart showed the ratio of IRE1α, TRAF2, p-ASK1 and p-JNK to β-actin at each group. (F). The expression levels of IRE1α, TRAF2, p-ASK1 and p-JNK were measured by western blot analysis. T24 cells were transfected with either control siRNA or with a specific IRE1α siRNA sequence at 50 nM for 24 h, and then treated with or without CXC195 before the subsequent experiments. (G–H). The bar chart showed the ratio of IRE1α, TRAF2, p-ASK1 and p-JNK to β-actin at each group. (I). The complexes of IRE1α/TRAF2 and IRE1α/ASK1 were precipitated by antibody against IRE1α first and then analyzed by western blot analysis for TRAF2 or ASK1. The protein levels of IRE1α, TRAF2, ASK1 and β-actin in whole cell lysate were analyzed by western blot analysis. (J). Densitometric analysis of effects of siRNA IRE1α on interactions of IRE1α with TRAF2 or ASK1 in CXC195 treated T24 cells. These data are means ± SEM. ($n = 6$, $^{*}P < 0.05$, $^{**}P < 0.01$ significantly different from the control group; $^{\#}P < 0.05$ significantly different from the CXC195 treatment group).

carcinoma HepG2 cells [16]. The subsequent events leading to effects of this drug on cancer cells is however not clear. In the present study we show, for the first time, that CXC195-induced apoptosis of human UC T24 cells is mediated by mitochondrial dysfunction and ER stress induced activation of JNK through the formation of an IRE1α-TRAF2-ASK1 complex.

The intrinsic or mitochondrial pathway of cell death is tightly modulated by proteins of the Bcl-2 family, which can be divided

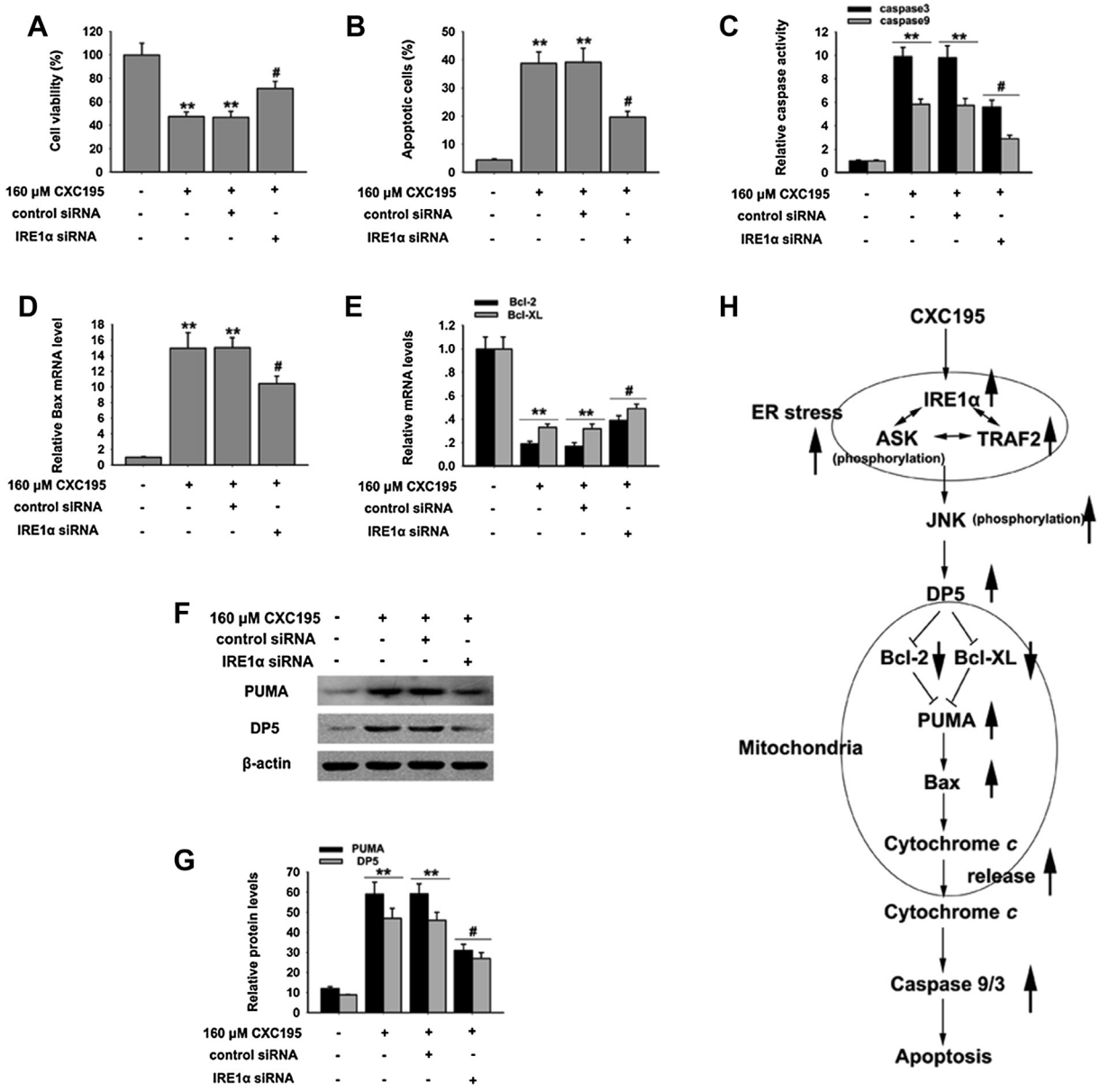

Fig. 4. Effect of IRE1α on mitochondrial-dependent apoptosis in CXC195 treated T24 cells. T24 cells were transfected with either control siRNA or with a specific IRE1α siRNA sequence at 50 nM for 24 h, and then treated with or without CXC195 before the subsequent experiments. (A). Effect of specific IRE1α siRNA on the cell viability of CXC195 treated T24 cells. (B). Effect of specific IRE1α siRNA on the level of apoptosis in CXC195 treated T24 cells. (C). Effect of specific IRE1α siRNA on the level of caspase3 and caspase9 activity in CXC195 treated T24 cells. (D–E). Effect of specific IRE1α siRNA on the mRNA levels of Bax, Bcl-2 and Bcl-XL in CXC195 treated T24 cells. (F–G). Effect of specific IRE1α siRNA on the protein levels of PUMA and DP5 in CXC195 treated T24 cells. These data are means ± SEM. (n = 6, *P < 0.05, **P < 0.01 significantly different from the control group; #P < 0.05 significantly different from the CXC195 treatment group).

into two groups: anti-apoptotic members, such as Bcl-2 and Bcl-XL; pro-apoptotic members which are further subdivided in multi-domain such as Bax and Bak, and BH3-only proteins, such as DP5 and PUMA [6]. Apoptosis starts with Bax translocation from the cytosol to the mitochondrial membrane, where it oligomerizes with Bak. The pore formed by Bax/Bak causes mitochondrial outer membrane permeabilization, allowing soluble proteins such as Cyt *c* to diffuse to the cytosol. The subsequent formation of the apoptosome leads to the activation of caspase 9 and caspase3, which mediated cell death. The BH3-only proteins induce apoptosis in a cell type- and stimulus-dependent pattern. These proteins are essential initiators of apoptosis by exerting their ability to bind and inhibit pro-survival Bcl-2 members and by directly activating of Bax and Bak [20]. Our results showed that decreased expression of anti-apoptotic Bcl-2 and Bcl-XL, and increased expression of pro-apoptotic Bax, PUMA and DP5 were observed in CXC195-treated T24 cells. In addition, activation of caspase3 and caspases9 were induced after CXC195 treatment. Furthermore, the amount of Cyt-c significantly was decreased in mitochondria whereas it was found to be increased in cytosol. Therefore, CXC195 might initiate intrinsic pathway which induced mitochondrial-dependent apoptotic signaling in T24 cells.

Activation of the JNK pathway has been shown to be a common phenomenon in stress-induced apoptosis in response to intracellular stresses such as treatment with anti-cancer agents (antimetabolites) [21]. Studies have shown that the JNK pathway plays an important role in the regulation of mitochondrial-dependent pro-apoptotic signal transduction [17]. Activation of the JNK pathway

promotes release of Cyto-c, activates Bax by phosphorylation [22] and up-regulates PUMA and DP5 [18,19]. This supported our results that activation of JNK was consistent with the release of Cyto-c, up-regulation of Bax, PUMA and DP5 in CXC195-treated T24 cells.

Previous studies also have shown that the JNK signaling pathway could be activated by ER stress following recruitment of TRAF2 by the IRE1 cytosolic kinase to form an IRE1α-TRAF2-ASK1 complex [7]. In the present study, the activation of IRE1α, ASK1 and TRAF2 were consistent with the activation of the JNK pathway suggesting that JNK was activated in response to CXC195-induced ER stress. The almost complete loss of JNK activation and CXC195-induced mitochondrial-dependent apoptosis caused by the inhibition of IRE1α strongly suggests that IRE1α constitutes an essential and nonredundant cell death-signaling pathway in response to CXC195 treatment. Furthermore, IRE1α was found to be associated with TRAF2 and ASK1 after treatment with CXC195, and this association complete lost after inhibition of IRE1α. These results suggest that CXC195-induced activation of the JNK pathway is mediated by formation of the IRE1α-TRAF2-ASK1 complex.

In summary, these results suggest that CXC195 induces apoptosis by the events shown in Fig. 4H. CXC195 induces the ER stress by the activation of IRE1α, which leads to activation of JNK via recruitment of TRAF2 and ASK1. Activation of JNK then activate DP5 and PUMA, inhibit Bcl-2 and Bcl-XL, and consequently induce mitochondrial- and caspase-dependent apoptosis.

Appendix A. Supplementary data

Supplementary data related to this article can be found at http://dx.doi.org/10.1016/j.bbrc.2015.03.064.

References

[1] A. Jemal, R. Siegel, J. Xu, E. Ward, Cancer statistics, 2010, CA Cancer J. Clin. 60 (2010) 277–300.
[2] J.E. Rosenberg, P.R. Carroll, E.J. Small, Update on chemotherapy for advanced bladder cancer, J. Urol. 174 (2005) 14–20.
[3] C.H. Chen, H.J. Yang, C.T. Shun, C.Y. Huang, K.H. Huang, H.J. Yu, Y.S. Pu, A cocktail regimen of intravesical mitomycin-C, doxorubicin, and cisplatin (MDP) for non-muscle-invasive bladder cancer, Urol. Oncol. 30 (2012) 421–427.
[4] I.M. Ghobrial, T.E. Witzig, A.A. Adjei, Targeting apoptosis pathways in cancer therapy, CA Cancer J. Clin. 55 (2005) 178–194.
[5] J. Wang, K. Hansen, R. Edwards, B. Van Houten, W. Qian, Mitochondrial division inhibitor 1 (mdivi-1) enhances death receptor-mediated apoptosis in human ovarian cancer cells, Biochem. Biophys. Res. Commun. (2014).
[6] R.J. Youle, A. Strasser, The BCL-2 protein family: opposing activities that mediate cell death, Nat. Rev. Mol. Cell. Biol. 9 (2008) 47–59.
[7] F. Urano, X. Wang, A. Bertolotti, Y. Zhang, P. Chung, H.P. Harding, D. Ron, Coupling of stress in the ER to activation of JNK protein kinases by transmembrane protein kinase IRE1, Science 287 (2000) 664–666.
[8] B. Yi, D. Liu, M. He, Q. Li, T. Liu, J. Shao, Role of the ROS/AMPK signaling pathway in tetramethylpyrazine-induced apoptosis in gastric cancer cells, Oncol. Lett. 6 (2013) 583–589.
[9] Z. Chen, X. Pan, A.G. Georgakilas, P. Chen, H. Hu, Y. Yang, S. Tian, L. Xia, J. Zhang, X. Cai, J. Ge, K. Yu, J. Zhuang, Tetramethylpyrazine (TMP) protects cerebral neurocytes and inhibits glioma by down regulating chemokine receptor CXCR4 expression, Cancer Lett. 336 (2013) 281–289.
[10] Y. Wang, Q. Fu, W. Zhao, Tetramethylpyrazine inhibits osteosarcoma cell proliferation via downregulation of NF-kappaB in vitro and in vivo, Mol. Med. Rep. 8 (2013) 984–988.
[11] K. Yu, Z. Chen, X. Pan, Y. Yang, S. Tian, J. Zhang, J. Ge, B. Ambati, J. Zhuang, Tetramethylpyrazine-mediated suppression of C6 gliomas involves inhibition of chemokine receptor CXCR4 expression, Oncol. Rep. 28 (2012) 955–960.
[12] X.C. Cheng, X.Y. Liu, W.F. Xu, X.L. Guo, Y. Ou, Design, synthesis, and biological activities of novel ligustrazine derivatives, Bioorg. Med. Chem. 15 (2007) 3315–3320.
[13] H. Liu, X. Wei, L. Chen, X. Liu, S. Li, X. Liu, X. Zhang, Tetramethylpyrazine analogue CXC195 protects against cerebral ischemia/reperfusion injury in the rat by an antioxidant action via inhibition of NADPH oxidase and iNOS expression, Pharmacology 92 (2013) 198–206.
[14] L. Chen, X. Wei, Y. Hou, X. Liu, S. Li, B. Sun, X. Liu, H. Liu, Tetramethylpyrazine analogue CXC195 protects against cerebral ischemia/reperfusion-induced apoptosis through PI3K/Akt/GSK3beta pathway in rats, Neurochem. Int. 66 (2014) 27–32.
[15] Y. Ou, X. Dong, X.Y. Liu, X.C. Cheng, Y.N. Cheng, L.G. Yu, X.L. Guo, Mechanism of tetramethylpyrazine analogue CXC195 inhibition of hydrogen peroxide-induced apoptosis in human endothelial cells, Biol. Pharm. Bull. 33 (2010) 432–438.
[16] Y. Wang, Q. Tu, W. Yan, D. Xiao, Z. Zeng, Y. Ouyang, L. Huang, J. Cai, X. Zeng, Y.J. Chen, A. Liu, CXC195 suppresses proliferation and inflammatory response in LPS-induced human hepatocellular carcinoma cells via regulating TLR4-MyD88-TAK1-mediated NF-kappaB and MAPK pathway, Biochem. Biophys. Res. Commun. (2014).
[17] C. Tournier, P. Hess, D.D. Yang, J. Xu, T.K. Turner, A. Nimnual, D. Bar-Sagi, S.N. Jones, R.A. Flavell, R.J. Davis, Requirement of JNK for stress-induced activation of the cytochrome c-mediated death pathway, Science 288 (2000) 870–874.
[18] C. Ma, C. Ying, Z. Yuan, B. Song, D. Li, Y. Liu, B. Lai, W. Li, R. Chen, Y.P. Ching, M. Li, dp5/HRK is a c-Jun target gene and required for apoptosis induced by potassium deprivation in cerebellar granule neurons, J. Biol. Chem. 282 (2007) 30901–30909.
[19] Y. Akazawa, S. Cazanave, J.L. Mott, N. Elmi, S.F. Bronk, S. Kohno, M.R. Charlton, G.J. Gores, Palmitoleate attenuates palmitate-induced Bim and PUMA up-regulation and hepatocyte lipoapoptosis, J. Hepatol. 52 (2010) 586–593.
[20] H. Kim, M. Rafiuddin-Shah, H.C. Tu, J.R. Jeffers, G.P. Zambetti, J.J. Hsieh, E.H. Cheng, Hierarchical regulation of mitochondrion-dependent apoptosis by BCL-2 subfamilies, Nat. Cell. Biol. 8 (2006) 1348–1358.
[21] J.M. Kyriakis, J. Avruch, Mammalian MAPK signal transduction pathways activated by stress and inflammation: a 10-year update, Physiol. Rev. 92 (2012) 689–737.
[22] B.J. Kim, S.W. Ryu, B.J. Song, JNK- and p38 kinase-mediated phosphorylation of Bax leads to its activation and mitochondrial translocation and to apoptosis of human hepatoma HepG2 cells, J. Biol. Chem. 281 (2006) 21256–21265.